THE JOURNAL OF BIOLOGICAL CHEMISTRY VOL. 286, NO. 26, pp. 22742–22749, July 1, 2011

Insecticidal Toxin Complex Proteins from *Xenorhabdus nematophilus*

STRUCTURE AND PORE FORMATION[*S]

Received for publication, February 1, 2011, and in revised form, April 12, 2011 Published, JBC Papers in Press, April 28, 2011, DOI 10.1074/jbc.M111.227009

Joel J. Sheets[‡1], Tim D. Hey[‡], Kristin J. Fencil[‡], Stephanie L. Burton[§], Weiting Ni[‡], Alexander E. Lang[¶], Roland Benz[‖], and Klaus Aktories[¶]**

*From the Departments of [‡]Biochemistry and Molecular Biology and [§]Biology, Dow AgroSciences, Indianapolis, Indiana 46268, [¶]Institut für Experimentelle und Klinische Pharmakologie und Toxikologie, Albert-Ludwigs-Universität Freiburg, D-79104 Freiburg, Germany, [‖]Rudolf-Virchow-Zentrum, Deutsche Forschungsgemeinschaft-Forschungszentrum für Experimentelle Biomedizin, Universität Würzburg, Versbacher Strasse 9, D-97078 Würzburg, Germany, and **School of Engineering and Science, Jacobs University Bremen, P. O. Box 750 561, D-28725 Bremen, Germany*

Toxin complexes from *Xenorhabdus* and *Photorhabdus* spp. bacteria represent novel insecticidal proteins. We purified a native toxin complex (toxin complex 1) from *Xenorhabdus nematophilus*. The toxin complex is composed of three different proteins, XptA2, XptB1, and XptC1, representing products from class A, B, and C toxin complex genes, respectively. We showed that recombinant XptA2 and co-produced recombinant XptB1 and XptC1 bind together with a 4:1:1 stoichiometry. XptA2 forms a tetramer of ~1,120 kDa that bound to solubilized insect brush border membranes and induced pore formation in black lipid membranes. Co-expressed XptB1 and XptC1 form a tight 1:1 binary complex where XptC1 is C-terminally truncated, resulting in a 77-kDa protein. The ~30-kDa C-terminally cleaved portion of XptC1 apparently only loosely associates with this binary complex. XptA2 had only modest oral toxicity against lepidopteran insects but as a complex with co-produced XptB1 and XptC1 had high levels of insecticidal activity. Addition of co-expressed class B (TcdB2) and class C (TccC3) proteins from *Photorhabdus luminescens* to the *Xenorhabdus* XptA2 protein resulted in formation of a hybrid toxin complex protein with the same 4:1:1 stoichiometry as the native *Xenorhabdus* toxin complex 1. This hybrid toxin complex, like the native toxin complex, was highly active against insects.

Xenorhabdus and *Photorhabdus* spp. are two bacterial genera belonging to the family Enterobacteriaceae, known to be associated with entomopathogenic nematodes (1–4) These bacteria represent potential sources for new genes encoding potent insecticidal toxins that could be put into plants as alternatives to *Bacillus thuringiensis* genes (5). Gene sequence analysis of *Xenorhabdus* and *Photorhabdus* bacteria show that these organisms contain a family of related toxin complex (*tc*)[2] genes located at different loci (6–9). The toxin complexes are composed of three different classes of protein components, which, according to ffrench-Constant *et al.* (10, 11), can be categorized as class A, B, and C proteins based upon sequence similarity and size. Class A proteins are very large, having a molecular mass of ~280 kDa. Class B proteins are ~170 kDa, and class C proteins are ~110 kDa. There are many different varieties of class A, B, and C proteins in both Gram-negative and Gram-positive bacteria (12–15).

From earlier studies, it has been suggested that class A proteins harbor the cytotoxic effects of the Tc toxins, whereas class B and C proteins modulate and enhance the toxicity of class A proteins (16). However, recently, we elucidated the molecular mechanism of the *Photorhabdus luminescens* Tc complex, which consists of the class A protein TcdA1, the class B protein TcdB2, and the class C protein TccC3 or TccC5 (17). These studies revealed that the class C proteins harbor the biological activity. It was shown that TccC3 and TccC5 are ADP-ribosyltransferases, which target the actin cytoskeleton by modification of actin and Rho GTPases, respectively (17). Moreover, these studies suggested that the class A protein TcdA1 of *P. luminescens* is most likely involved in the uptake of the enzyme component into target cells (18).

Here we analyzed the structure and stoichiometric composition of a toxin complex from *Xenorhabdus nematophilus* that is largely related to the Tc complex from *P. luminescens* mentioned above. We found that native *Xenorhabdus* toxin complex 1 is composed of three proteins (XptA2, XptB1, and XptC1) representing class A, B, and C proteins combined in a respective 4:1:1 stoichiometry. Using individual purified recombinant protein components of the *Xenorhabdus* and *Photorhabdus* toxin complexes, we demonstrated that a fully active toxin complex requires the presence of all three class A, B, and C proteins and that class B and C proteins from *Photorhabdus* (TcdB2 and TccC3) can substitute for the B and C proteins from *Xenorhabdus* to form an active hybrid toxin complex that has greater insecticidal activity than the native toxin complex.

* This work was supported by German Science Foundation Deutsche Forschungsgemeinschaft (DFG) Grant AK6/22-1 (to K. A.), the excellence cluster Centre for Biological Signalling Studies (BIOSS) (to K. A.), and DFG Grant SFB487 TP5 (to R. B.).

[S] The on-line version of this article (available at http://www.jbc.org) contains supplemental Fig. S1.

[1] To whom correspondence should be addressed: Dept. of Biochemistry and Molecular Biology, Dow AgroSciences, 9330 Zionsville Rd., Indianapolis, IN 46268. Fax: 317-337-3228; E-mail: jjsheets@dow.com.

[2] The abbreviations used are: Tc, toxin complex; SEC, size exclusion chromatography; SPR, surface plasmon resonance; GI_{50}, concentration required to reduce growth by 50%.

EXPERIMENTAL PROCEDURES

Purification and Characterization of Native Xenorhabdus Toxin Complexes—Cell pellets obtained from a 2-liter culture after overnight incubation of the *X. nematophilus* bacteria were suspended in 50 mM Tris-HCl, pH 8.0, 100 mM NaCl, 1 mM DTT, 10% glycerol, and 0.6 mg/ml lysozyme. A small amount of glass beads (0.5-mm diameter) was added, and cells were disrupted by sonication. Broken cells were then centrifuged at 48,000 × *g* for 60 min at 4 °C, supernatant was collected, a bacterial protease inhibitor mixture added (Sigma), and the solution was dialyzed against 25 mM Tris-HCl, pH 8.0 overnight. The protein was then loaded onto a Q Sepharose XL (1.6 × 10 cm) anion exchange column. Bound proteins were eluted using a linear 0–1 M NaCl gradient in 10 column volumes. The high molecular weight toxin complexes eluted in the early fractions and were concentrated and loaded onto a Superose 200 size exclusion column (1.6 × 60 cm) (GE Healthcare) using 50 mM Tris-HCl, 100 mM NaCl, 5% glycerol, 0.05% Tween 20, pH 8.0. The large molecular weight proteins eluting from the column were brought to 1.5 M ammonium sulfate concentration and loaded onto a phenyl Superose (0.5 × 5-cm) hydrophobic interaction column. Proteins were eluted using a decreasing linear gradient of 1.5- 0 M ammonium sulfate in 25 mM Tris-HCl, pH 8.0 over 20 column volumes. The toxin complexes eluted together as a broad peak at low salt concentration. The proteins were dialyzed overnight against 25 mM Tris-HCl and loaded onto a high resolution Mono Q (0.5 × 5-cm) anion exchange column. Two separate toxin complexes were resolved with base-line resolution using a linear gradient of 0–1 M NaCl in 25 mM Tris-HCl obtained in 20 column volumes (see Fig. 1). The proteins were identified by N-terminal amino acid sequencing and matrix-assisted laser desorption/ionization time-of-flight (MALDI-TOF) mass spectrometry analysis. Purification of recombinant XptA2 and co-expressed XptB1 + XptC1 and TcdB2 + TccC3 were done using similar chromatographic procedures.

Relative Mass Comparison by Size Exclusion Chromatography (SEC)—XptA2 (0.5 mg/ml) was incubated overnight at 4 °C with the following: 1) XptB1 + XptC1 (0.5 mg/ml each) in running buffer consisting of 25 mM Tris-HCl, pH 8.0, 5% glycerol, 0.05% Tween 20 or 2) an equal volume of running buffer only (control). To subsequently separate XptA2 from the unbound B and C proteins, the mixtures were applied to a Superdex 200 10/30 gel filtration column (GE Healthcare).

Electrophoresis—Analysis of proteins was done by sodium dodecyl sulfate-polyacrylamide gel electrophoresis (SDS-PAGE) (19) using 4–20% Tris-glycine polyacrylamide gels (Bio-Rad). Native PAGE was conducted for the electrophoretic mobility shift assays using precast NuPAGE® Novex 3–8% Tris-acetate gels (Invitrogen) and applying 150 V for 3 h.

Surface Plasmon Resonance—The binding of proteins was measured by surface plasmon resonance (SPR) using a Biacore 3000 instrument. Briefly, the proteins were immobilized onto the surface of a dextran/gold CM-5 or CM-4 Biacore chip following the manufacturer's recommended amine coupling procedure using 1-ethyl-3-(3-dimethylaminopropyl)carbodiimide hydrochloride and *N*-hydroxysuccinimide. Remaining free reactive esters were blocked with ethanolamine. For the analysis, the buffer flow rate was 30 μl/min using HPS-EP buffer (10 mM HEPES, pH 7.4, 0.15 M NaCl, 3 mM EDTA, 0.005%, Tween-20) (Biacore). Association of XptB1-XptC1 with the immobilized XptA2 was measured for 200 s, and dissociation was also measured for 200 s by flowing buffer in the absence of XptB1-XptC1 protein over the immobilized XptA2. A "blank" surface was prepared using 1-ethyl-3-(3-dimethylaminopropyl)carbodiimide hydrochloride and *N*-hydroxysuccinimide and blocking with ethanolamine using the same procedure as describe above but without any protein. Signals from the blank surface were subtracted from the signal from the surface containing the immobilized proteins.

For measurement of binding to insect gut binding proteins, brush border membrane vesicles were prepared by method of Wolfersberger (20) from last instar *Heliothis zea* insect larvae. The vesicles were solubilized with CHAPS detergent (2% final) in 20 mM Tris, pH 7.5, 1 mM EDTA, 1 mM $MgSO_4$, 0.01% NaN_3, and 10% glycerol with protease inhibitors. Following 1 h of gentle mixing at 4 °C, the mixture was centrifuged for 1 h at 100,000 × *g* at 4 °C, and the supernatant was collected, filtered through a 0.2-μm membrane, and loaded onto a Mono Q (0.5-cm-diameter, 5-cm-long) anion exchange column (GE Healthcare) equilibrated in solubilization buffer containing 1% CHAPS. The proteins were eluted with a linear gradient from 0 to 500 mM KCl in solubilization buffer containing 1% CHAPS. Samples were kept at 4 °C and used the day of preparation. XptA2 was immobilized on a CM-5 chip, and each fraction was tested for binding. The fraction showing the strongest binding was then immobilized onto a CM-4 chip, and various concentrations of XptA2 were flowed over the immobilized XptA2 to measure binding.

Insect Bioassays—Proteins were tested for insecticidal activity in bioassays conducted with neonate lepidopteran larvae on artificial insect diet. *Helicoverpa zea* Boddie and *Heliothis virescens* larvae came from a colony maintained by a commercial insectary (Benzon Research Inc., Carlisle, PA). The bioassays were conducted in 128-well plastic trays (C-D International, Pitman, NJ). Each well contained 1.0 ml of multispecies Lepidoptera diet (Southland Products, Lake Village, AR). A 40-μl aliquot of sample was delivered by pipette onto the 1.5-cm^2 diet surface of each well (26.7 μl/cm^2). Eight wells were treated for each insect per replicate. Within a few hours of eclosion, individual larvae were deposited on the treated diet. The infested wells were then sealed and held under controlled environmental conditions (28 °C, ~40% relative humidity, 16:8-h light:dark photoperiod). After 5 days, the total number of insects exposed to each protein sample, the number of dead insects, and the weight of surviving insects were recorded. Average weight and S.E. (95% confidence interval) for the insects were calculated from these data. A logistic two-parameter regression was used to fit growth inhibition to log-transformed protein concentration; GI_{50} (concentration required to reduce growth by 50%) values and 95% confidence intervals were estimated for each insect strain treated with each protein. All analyses were conducted in JMP 9.0 (SAS Institute Inc., Cary, NC).

Black Lipid Bilayer Experiments—The method used for preparation of black lipid bilayers has been described previ-

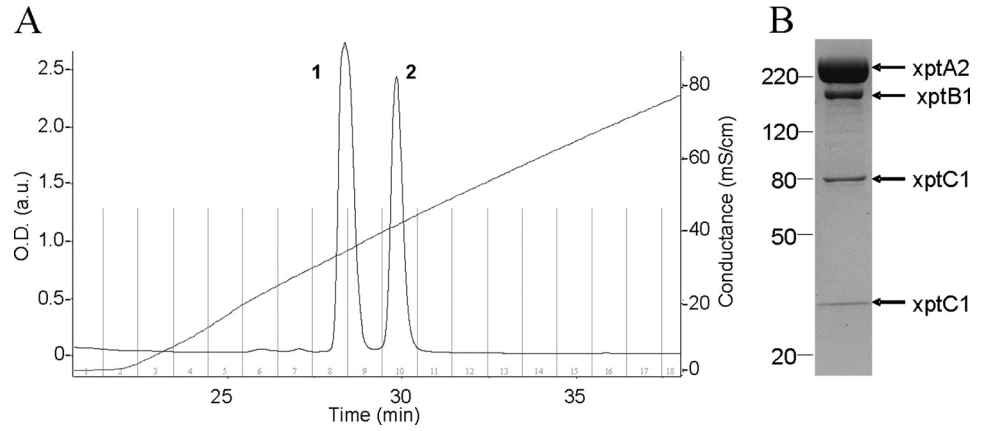

FIGURE 1. **Final chromatographic resolution of *Xenorhabdus* toxin complexes.** *A*, high resolution anion exchange chromatogram (Mono Q, 0.5 × 5 cm) of high molecular weight fractions off the hydrophobic interaction column. The *two peaks* represent *A* at 280 nm, and the *upward sloping line* is conductance (millisiemens (*mS*)/cm). Peak *1* is *Xenorhabdus* toxin complex 1, and peak *2* is *Xenorhabdus* toxin complex 2. Analysis of the second peak revealed a second toxin complex of completely different structure that will be described in more detail in a future report. *a.u.*, absorbance units. *B*, SDS-PAGE of purified native toxin complex 1 from *X. nematophilus* under reducing and denaturing conditions. *Numbers* represent molecular weight from BenchMark™ markers. The relative staining intensity of the three major bands, when adjusted for protein size, is 4:1:1 for XptA2, XptB1, and XptC1, respectively.

ously (21, 22). The experimental setup consisted of a Teflon chamber divided into two compartments by a thin wall and connected by a small circular hole with a surface area of about 0.4 mm^2. The aqueous solutions on both sides of the membrane were buffered with 10 mM MES-KOH to pH 6. Membranes were formed by spreading a 1% solution of diphytanoyl phosphatidylcholine dissolved in *n*-decane across the hole. After the membranes turned black, XptA1 was added to one side of the membrane, the cis side. The temperature was maintained at 20 °C during experiments. Membrane conductance was measured after application of a fixed membrane potential by using a pair of silver/AgCl electrodes (with salt bridges) connected in series to a voltage source and a homemade current amplifier made with a Burr Brown operational amplifier. The amplified signal was monitored on a storage oscilloscope (OWON, Chorley, UK) and recorded on a strip chart recorder (Rikadenki, Freiburg, Germany).

RESULTS AND DISCUSSION

Purification of Native Toxin Complex—Fractionation and purification of large molecular mass proteins from *X. nematophilus* cells resulted in the isolation of multiple proteins that eluted in two base-line separated peaks in the final anion exchange chromatography step (Fig. 1*A*). Analysis of the proteins contained in the first eluting peak by SDS-PAGE showed it to consist of three major protein components of 280, 170, and 77 kDa and one minor protein component of ~30 kDa (Fig. 1*B*). The 280-kDa band exhibited considerably greater staining intensity by Coomassie Blue dye compared with the other protein bands even when taking into consideration its greater mass. Densiphotometric analysis of the three major bands, when adjusted for protein size, indicated that the ratio of the 280- to 170- to 77-kDa protein bands is 4:1:1.

Analysis of the individual protein bands by MALDI-TOF showed a complete match of the 280-kDa protein to XptA2 and a complete match of the 170-kDa protein to XptB1 (supplemental Fig. S1). Tryptic digests of the 77-kDa band matched residues located in the N-terminal ⅔ portion of XptC1 but no farther, suggesting that the C-terminal ⅓ portion of this protein

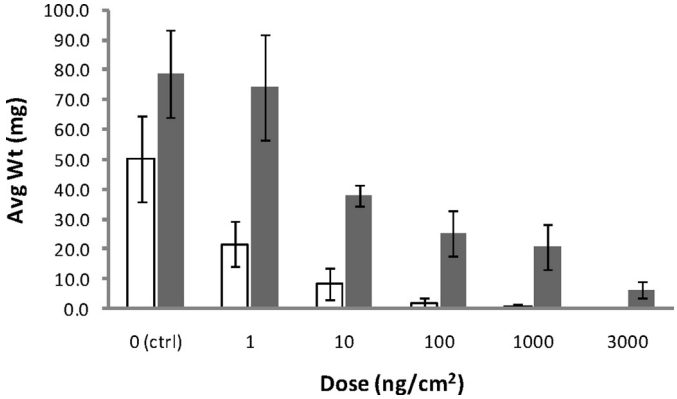

FIGURE 2. **Biological activity of *Xenorhabdus* native toxin complex 1.** Shown is the ability of the toxins to inhibit growth of two different insect larvae, *Helicoverpa zea* Boddie (*open bars*) and *Heliothis virescens* (*solid bars*), over a 5-day time period when the amount of purified toxin complex protein (in ng/cm^2) was applied to the top surface of artificial insect diet. Weights are compared with insects receiving protein buffer alone. $n = 24–36$ insects tested per dose. *Error bars* represent S.E. (95% confidence interval). *ctrl*, control; *Avg Wt*, average weight.

was probably missing, which is consistent with the protein migrating on SDS-PAGE with an apparent molecular mass of 77 kDa (Fig. 1*B*) as opposed to ~110 kDa for the full-length gene product. The minor band migrating with an apparent molecular mass of ~30 kDa was analyzed by MALDI and determined to be the C-terminal fragment of XptC1. Thus, it appears that XptC1 is proteolytically processed either by enzymes located in *X. nematophilus* or by the toxin complex protein itself and that these three proteins associate together to form a large complex.

Biological Activity of Toxin Complex—The biological activity of toxin complex 1 was measured by applying 1, 10, 100, 1,000, or 3,000 ng/cm^2 purified protein onto the surface of insect diet and allowing the insects to feed for 5 days. The weight of insects was taken as a readout (Fig. 2). Toxin complex 1 was active against both insects but with the greatest activity against *Helicoverpa zea*. The average weight of *Helicoverpa zea* was significantly reduced with a toxin complex 1 concentration of 1 ng/cm^2 compared with the average weights of treated insects

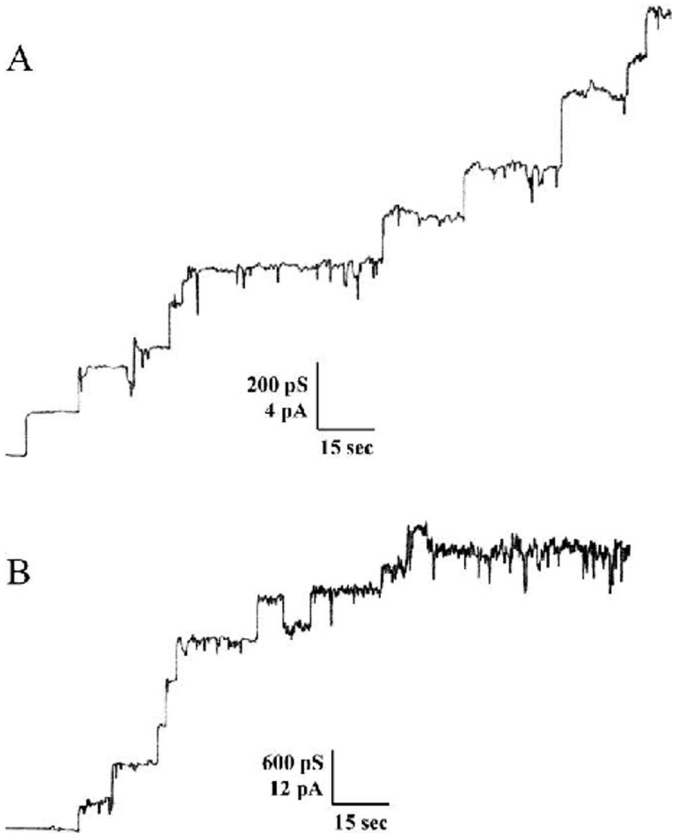

FIGURE 3. **Current recordings of diphytanoyl phosphatidylcholine/*n*-decane membranes of channels formed by XptA1.** 5 min after the start of the recordings, XptA2 was added to the cis side of different membranes. The aqueous phase contained 0.15 M KCl (*A*) or 1.0 M KCl (*B*) and 10 mM MES-KOH, pH 6. The applied membrane potential was 20 mV; $T = 20$ °C. *pS*, picosiemens.

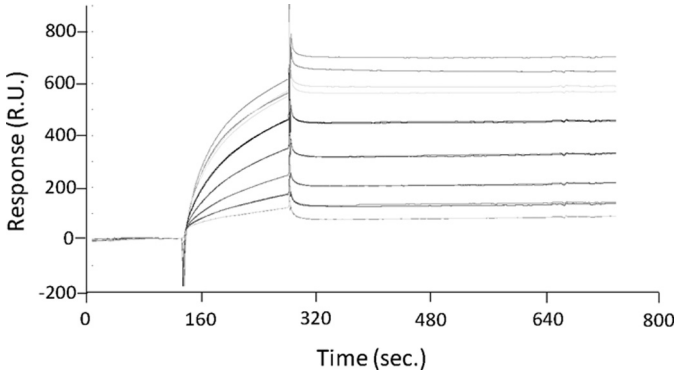

FIGURE 4. **Binding of XptA2 to solubilized brush border membrane fraction from *Helicoverpa zea* larvae.** XptA2 was added at 2-fold increasing concentrations ranging from 1.5 to 100 nM to solubilized insect midgut membrane fractions immobilized onto a CM-4 chip. Binding was measured by SPR. *RU*, resonance units.

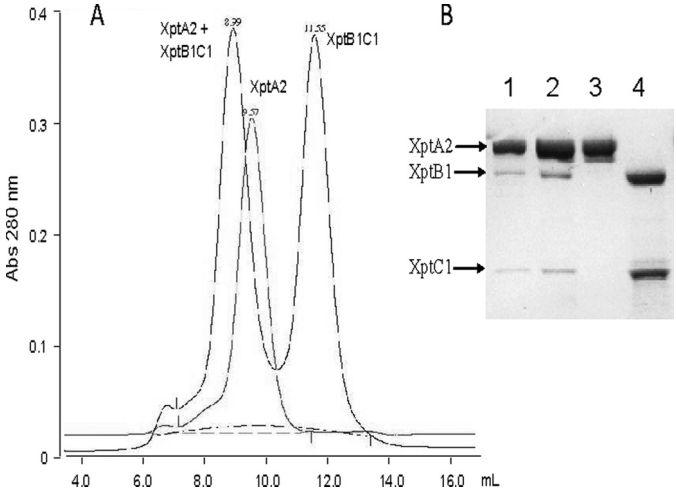

FIGURE 5. **Analytical SEC comparison of elution volumes for XptA2 alone (*single peak*) and XptA2 + $XptB1_{xwi}$-$XptC1_{xwi}$ (*double peak*).** *A*, the earlier elution of XptA2 to which XptB1-XptC1 was added (compared with XptA2 alone) from the Superdex 200 10/30 column shows that incubation of XptB1-XptC1 with XptA2 results in a size increase of the complex and indicates that the XptB1-XptC1 complex is binding to XptA2. *Abs*, absorbance. *B*, SDS-PAGE of SEC samples. *Lane 1*, native *Xenorhabdus* toxin complex 1 control having all three proteins, XptA2, XptB1, and XptC1; *lane 2*, XptA2 + XptB1-XptC1, 8.99-ml eluting peak in Fig. 3*A*; *lane 3*, XptA2, 9.57-ml eluting peak in Fig. 3*A*; *lane 4*, XptB1-XptC1, 11.55-ml eluting peak in Fig. 3*A*.

on the buffer-only control. The GI_{50} of toxin complex 1 was 0.3 ng/cm^2 for *Helicoverpa zea* and 48.5 ng/cm^2 for *H. virescens*.

Pore Formation by XptA2 in Black Lipid Membranes—Recently, it has been suggested that the XptA2-related toxin component TcdA1 from *P. luminescens* is involved in toxin uptake by forming pores in cell membranes (17). Therefore, we studied the effects of purified XptA1 in black lipid membranes. As shown in Fig. 3, addition of the toxin component to the cis side of the membrane increased the membrane current in a stepwise manner. The single channel conductance in the presence of 0.15 and 1 M KCl was ~100 and ~400 picosiemens, respectively. These data indicate that the XptA2 component exhibits strong membrane activity and forms pores.

Xenorhabdus Toxin Complex Binds to Solubilized Insect Gut Membranes—Midgut membranes from *Helicoverpa zea* larvae were solubilized and immobilized onto a Biacore chip, and the binding of native *Xenorhabdus* toxin was measured by SPR. The results (Fig. 4) show increased binding as increased concentrations of *Xenorhabdus* toxin complex 1 were flowed over the immobilized gut membrane protein fraction. When the binding curves were fitted to a Langmuir isotherm model for 1:1 interaction between the analyte and the immobilized ligand, a K_d value of 0.2 nM was obtained for the binding affinity.

Recombinant XptA2 Forms Tetramers—The gene *xptA2*, encoding the large class A protein, was cloned and expressed in *Escherichia coli*. The resulting recombinant XptA2 protein was purified with techniques similar to those used to purify the native toxin complex proteins, resulting in a single protein band with an apparent molecular mass of 280 kDa when analyzed by SDS-PAGE (Fig. 5*B*, *lane 3*). When analyzed by native PAGE, XptA2 migrated significantly less distance in the gel than the highest molecular mass standard of 669 kDa, which is consistent with XptA2 existing as a high molecular mass oligomer (data not shown). The recombinant XptA2 was passed though a calibrated Superdex 200 SEC column to determine its approximate molecular mass (Fig. 5*A*). Recombinant XptA2 eluted from the SEC column at 9.57 ml, significantly earlier than the highest molecular mass standard (670 kDa), which eluted at 9.96 ml (not shown). Based upon an extrapolation of the calibration curve from the sizing column, the molecular mass of recombinant XptA2 was estimated to be ~1,200 kDa. This suggests that the XptA2 protein, in the absence of class B and C proteins, forms a tetramer, which would have a combined

molecular mass of 1,120 kDa, closely agreeing with this result. The formation of a tetramer is consistent with a previously reported proposed tetramer structure for TcdA1 from *Photorhabdus* (16) and the more recent three-dimensional structural characterization of XptA1 revealing a tetramer with a cagelike structure (23).

Complexes Formed by Recombinant Toxin Components—Next, recombinant XptB1 and XptC1 proteins were co-produced together in *E. coli* and purified to apparent homogeneity. When analyzed by SEC, XptB1 and XptC1 eluted together as a single symmetrical peak at a volume corresponding to an apparent molecular size of ~250 kDa, the sum of the masses of the two proteins together (Fig. 5*A*). On native PAGE, the two proteins formed a single band, indicating these two proteins exist as a binary complex (data not shown). Similar to what was observed in the native toxin complex, when analyzed by SDS-PAGE, the recombinant class C protein XptC1 exists as a cleaved 77-kDa protein in this preparation with a very small amount of the C-terminal 30-kDa fragment also present. N-terminal sequencing of the C-terminal fragment revealed that the cleavage site is identical to the site of cleavage of XptC1 when it is isolated from the native toxin complex 1 ($Arg^{679} \downarrow Phe^{680}$). The cleavage site is immediately after the site where the amino acid sequence similarities of different class C proteins from various organisms radically diverge.

To test whether or not the three recombinant proteins (XptA2, XptB1, and XptC1) together are capable of forming a larger complex, the three recombinant proteins were analyzed by SEC. When excess amounts of XptB1 + XptC1 were incubated with XptA2 and the mixture was subsequently analyzed by SEC, two peaks eluted from the column (Fig. 5*A*). The first peak eluted at a volume less than where XptA2 alone eluted (8.99 *versus* 9.57 ml), indicating that these three proteins now associate together to form a larger complex. The size of this larger complex was difficult to determine because we did not have molecular mass standards this large with which to compare, but apparently the molecular mass of the complex is now greater than the estimated size of 1,200 kDa for XptA2 alone because the newly formed complex eluted at a lower volume than XptA2 alone. Additionally, under these same conditions, the native toxin complex 1 eluted at nearly the same volume as the recombinant protein mixture (8.92 ml; chromatogram not shown), indicating the similar size of the recombinant and native complexes.

The two peaks that eluted from the SEC were then analyzed by SDS-PAGE to determine the content of each fraction (Fig. 5*B*). The earlier eluting peak (8.99 ml) obtained after incubating XptA2 with XptB1 + XptC1 contained all three proteins (*lane 2*), which further indicated that all three proteins are now associated together as is the case with the native *Xenorhabdus* toxin complex 1 (*lane 1*). Based upon the intensity of Coomassie Blue staining, XptA2 is the vastly predominant protein component. The level of staining of XptB1 and XptC1 showed both proteins to be present at an approximate 1:1 ratio, taking into consideration the differences in molecular weight of these proteins (*lanes 1*, *2*, and *4*). Thus, XptB1 and XptC1 apparently bind together as a tightly associated 1:1 binary complex and when added to XptA2 form a larger complex composed of all three proteins but with XptA2 in greater quantity than either XptB1 or XptC1. The trailing peak from the SEC column (11.55 ml) consisted of the excess XptB1 and XptC1proteins, which had not bound to the available XptA2 (*lane 4*).

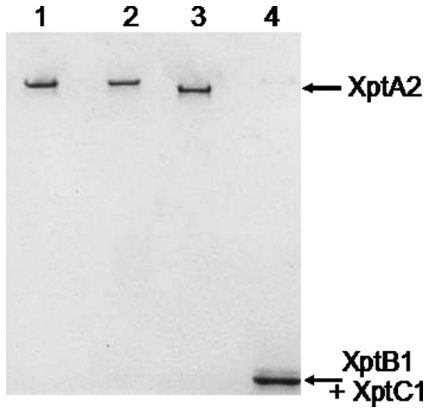

FIGURE 6. **Native PAGE of electrophoretic mobility shift assay of XptC1-XptB1 binding to XptA2.** *Lane 1*, native toxin complex 1; *lane 2*, XptA2 + XptB1-XptC1; *lane 3*, XptA2; *lane 4*, XptB1-XptC1. Incubation of XptA2 with XptB1-XptC1 caused decreased migration of XptA2 into the native gel, indicating that a change in size and/or pI had occurred. The gel was stained with Coomassie Blue.

Analysis of Toxin Complex by Native PAGE—To further substantiate that the recombinant proteins XptA2, XptB1, and XptC1 bind together to form a tightly associated complex, electrophoretic mobility shift assays were conducted using these three proteins. When XptA2 was analyzed by native PAGE, a single protein band of high apparent molecular mass was observed (Fig. 6, *lane 3*), but this protein band migrated farther in the gel than the *Xenorhabdus* native toxin complex 1 (Fig. 6, *lane 1*). When XptA2 was mixed with the binary complex of XptB1 + XptC1, separated from the excess XptB1 + XptC1 by SEC, and then analyzed by native PAGE, a single high molecular weight band was observed that electrophoretically migrated to the same distance as native *Xenorhabdus* native toxin complex 1 and less than the distance by XptA2 alone (Fig. 6, *lane 2*). The observation that a single newly formed band was formed that migrated a lesser distance in the gel compared with XptA2 by itself is consistent with the formation of a larger protein complex.

Surface Plasmon Resonance Studies—To further characterize the interaction of XptB1 + XptC1 with XptA2, we measured the binding of these proteins by SPR. When XptA2 was immobilized onto the chip and the co-expressed purified XptB1-XptC1 proteins were flowed over its surface, we observed initial rapid binding of the B-C proteins to the immobilized XptA2. This response was detected by an initial rapid increase in the resonance units followed by a slower rate of binding (Fig. 7). We did not observe any measurable dissociation of XptB1 + XptC1 proteins when only running buffer was subsequently flowed over the immobilized XptA2 (Fig. 7). Apparently, the binding of XptB1 + XptC1 proteins to XptA2 is exceedingly strong, and the very low rate of dissociation prevented us from determining the K_d for binding using this procedure. Binding of XptB1 + XptC1 to XptA2 protein is so tight that once bound they are essentially

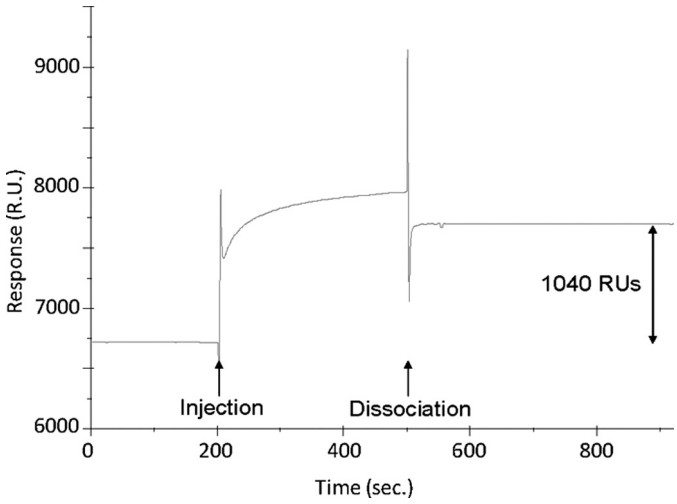

FIGURE 7. **SPR sensorgram of XptC1-XptB1 binding to XptA2 surface.** 50 μl of a 1.7 mg/ml solution of XptB1-XptC1 was injected over an XptA2 surface of ~7,100 resonance units (7.1 ng). The flow rate during injection was 10 μl/min. The running buffer was composed of 50 mM Tris-Cl, 100 mM NaCl, 10% glycerol, and 0.05% Tween 20, pH 8. The sensorgram represents blank-subtracted data. *RU*, resonance units.

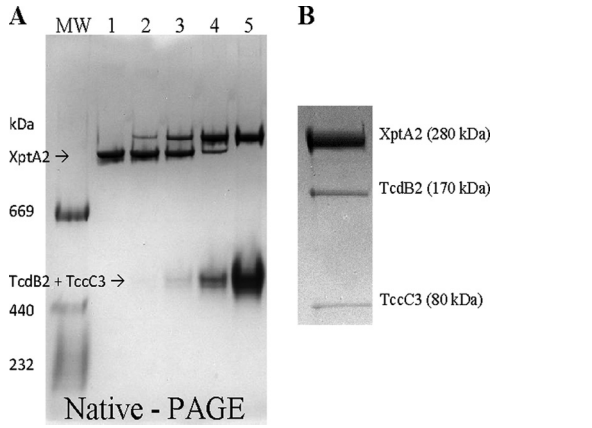

FIGURE 8. *A*, native PAGE of a titration of XptA2 with TcdB2-TccC3. *Lanes 1-5* represent 0, 0.1, 0.25, 1.0, and 4.0 μM TcdB2-TccC3 added to 1 μM XptA2, respectively. *B*, SDS-PAGE under denaturing and reducing conditions of high molecular weight toxin complex after being cut from the native gel (*A*, *lane 5*) and electroeluted. Densiphotometry readings of the bands gave a 4:1:1 ratio of XptA2 to TcdB2 to TccC3 when taking into account the difference in molecular weight of the bands.

irreversibly associated with the immobilized XptA2 because we were not able to find conditions that dissociate these proteins that are not so harsh as to denature XptA2.

XptA2 Forms Complex with P. luminescens TcdB2-TccC3 Fusion Toxins—To determine how receptive XptA2 is to bind class B and C proteins from different organisms, purified recombinant TcdB2 and TccC3 proteins from *P. luminescens* strain W-14 were used to measure their interaction with XptA2. These represent two entirely different B and C proteins compared with XptB1 and XptC1 with less than 54% amino acid sequence identity. When *tcdB2* and *tccC3* were co-expressed together in *E. coli* and the proteins were purified, we found that TccC3 was also cleaved into 77-kDa N-terminal and 30-kDa C-terminal products. The site of cleavage ($Leu^{678} \downarrow Met^{679}$) is equivalent with that of XptC1. An electrophoretic mobility shift assay was conducted to measure the interaction of these proteins together by titrating XptA2 with TcdB2-TccC3 (Fig. 8*A*). As TcdB2-TccC3 was added to XptA2, a higher molecular weight band having lesser electrophoretic migration in the native gel compared with XptA2 appeared. This newly formed band also correspondingly increased in amount as the concentration of TcdB2-TccC3 added to XptA2 was increased. We also observed a concomitant decrease in the amount of the band corresponding to XptA2 alone. This transitioning of banding patterns on the native PAGE gel represents the formation of a hybrid toxin complex. Fig. 8*A*, *lane 5*, shows the condition in which all of the XptA2 was in the lesser migrating complex due to addition of TcdB2-TccC3 at saturating amounts, leaving no free XptA2. When this high molecular weight protein band was cut from the native PAGE gel, electroeluted, and analyzed by SDS-PAGE under denaturing conditions, we observed the presence of three different bands corresponding to XptA2, TcdB2, and the N-terminal ⅔ portion of TccC3 (Fig. 8*B*). Densiphotometry analysis of the staining intensity of these bands, taking into consideration their differences in molecular weights, gave a 4:1:1 stoichiometry for the amount of XptA2 to TcdB2 to TccC3. Thus, there is a 1:1 ratio of TcdB2 and TccC3, which bind together, and this binary complex of proteins binds to four XptA2 proteins as was observed for XptB1-XptC1 with XptA2 in the *Xenorhabdus* native toxin complex 1. The 30-kDa C-terminal fragment of TccC3, if present, was too low in concentration to detect by Coomassie Blue staining.

TABLE 1

Biological activity of XptA2 against *Helicoverpa zea* larvae in presence or absence of E. coli lysate expressing TcdB2-TccC3

Numbers in the column headed XptA2 represent the concentration of this protein in ng/cm^2 that is placed on top of the diet prior to addition of insects. The + or − symbol in the column headed TcdB2 + TccC3 lysate indicates whether a 1:10 dilution of an *E. coli* cell lysate co-expressing these two proteins was added to the diet in addition to the indicated concentration of XptA2. The number of dead larvae is from $n = 8$. Percent growth inhibition is the mean weight of eight treated larvae compared with the mean weight of eight larvae receiving only water as the diet treatment.

		Insect activity	
XptA2	TcdB2 + TccC3 lysate	No. dead	Growth inhibition
ng/cm²			*%*
2,500	−	0	80
500	−	0	32
2,500	+	4	100
500	+	7	100
100	+	7	100
20	+	4	100
4	+	1	98
0	+	0	16

Heterologous Toxin Complex of XptA2 and TcdB2-TccC3 Possesses Insecticidal Activity—To demonstrate that the binding of TcdB2-TccC3 to XptA2 is a physiologically significant event, we tested the effects of the combination of toxin components in insects. As shown in Table 1, when fed to first instar *Helicoverpa zea* larvae in a top loaded artificial diet, purified recombinant XptA2 alone resulted primarily in stunting of larval growth. The maximum growth inhibition was 80% at the highest concentration tested (2,500 ng/cm^2) and was only 32% growth inhibition when tested at 500 ng/cm^2. In contrast, when *E. coli* lysate from bacteria co-producing TcdB2 and TccC3 was mixed with purified XptA2 and fed to the larvae in a top load

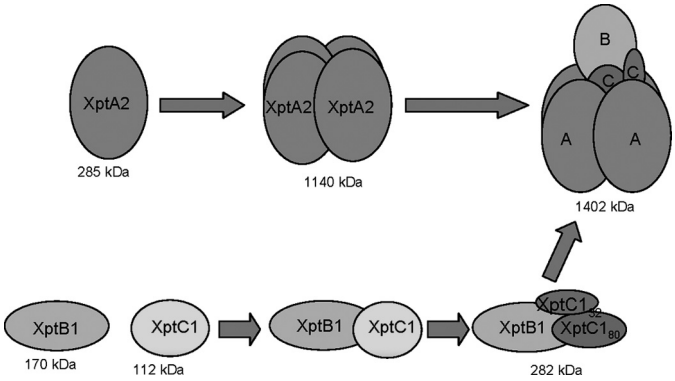

FIGURE 9. **Putative model of complete native toxin complex 1 from *X. nematophilus*.** The large 285-kDa XptA2 protein forms a homotetramer, resulting in a 1,140-kDa complex. The XptB1 and XptC1 proteins bind together to form a 1:1 dimer. Either after they bind together or just prior to binding together, the 112-kDa XptC1 protein is cleaved into an N-terminal 80-kDa fragment and a 32-kDa C-terminal fragment, both still bound to XptB1. The mechanism of cleavage is not known. This complex then binds to the tetrameric XptA2 to form the complete 1,402-kDa toxin complex. The exact location where XptB1 and XptC1 proteins bind to XptA2 is not known but is positioned on top of the complex for illustrative purposes.

diet, we obtained 100% larvae growth inhibition at XptA2 concentrations as low as 20 ng/cm^2 and with significant insect mortality at this and higher concentrations. Thus, in the presence of TcdB2 and TccC3, the insecticidal activity of XptA2 was increased by more than 100-fold. Feeding insect larvae the lysate containing TcdB2 and TccC3 without XptA2 resulted in only minor (16%) growth inhibition compared with that of non-transformed bacterial lysates, showing that these two proteins have little or no effect on the larvae by themselves. Thus, these data are largely in agreement with our recent findings that the major toxicity of Tc toxins is attributed to component TccC3 (17, 18) and suggest that XptA2 allows the uptake of the toxin component from *P. luminescens*. Moreover, comparing the activity of this hybrid toxin complex with the biological activity of the *Xenorhabdus* native toxin complex 1 (compare Fig. 2 with Table 1), we obtained greater growth inhibition at 4 ng/cm^2 XptA2 in the presence of TcdB2 + TccC3 than what occurs with 100 ng/cm^2 complete *Xenorhabdus* native toxin complex 1, although both toxins are highly active. Thus, the ability to use different class B and C proteins from different bacterial sources to potentiate the biological activity of different class A proteins opens the possibility to greatly expand both the spectrum and activity of this family of toxins.

Conclusions—Based upon the results presented in this study, we propose a model of the structure for the toxin complex (Fig. 9). In this model, the class A protein (XptA2) forms a 1,140-kDa tetramer. We have drawn these proteins simply as *ovals* grouped together where they line up in a parallel fashion, forming a tube with two contacts between adjacent proteins. This arrangement approximates the 25-Å-resolution structure observed from studies using transmission electron microscopy of negatively stained XptA2 (23). The class B and C proteins (XptB1 and XptC1) form a strongly associated binary complex with the C-terminal portion of XptC1 truncated and only weakly associated with the complex. It is believed that this complex of full-length XptB1 and both sections of XptC1 then strongly bind to the tetrameric XptA2 to form the complete and fully active toxin complex.

The class C protein components from *P. luminescens* have been shown to be ADP-ribosyltransferases that modify actin and RhoA proteins, resulting in clustering of actin (17, 18). We have not determined the activity of class C proteins from *Xenorhabdus* toxin complexes. Our studies of XptA2 showed this component to strongly bind solubilized insect midgut membrane fractions and to be able to form pores in artificial membranes. It is likely that this component is involved in translocation of the class C toxin component in the intoxication process. The site on the tetrameric class A protein where the B-C proteins bind is not known, but it is tempting to assume that the site is in the middle of the tetramer where a symmetrical channel would presumably exist.

The finding that the class A components are capable of delivery of Tc toxins from different types of bacteria will largely facilitate studies on this family of toxins. Moreover, the interchangeability of the toxins might be of great benefit for the development of novel biological insecticides.

Acknowledgments—We thank Scott Bintrim for supplying the culture of native X. nematophilus for purification of the native toxin complexes and Tamar Finley for help with the purification of the proteins described in these studies. We also thank Ping Xu for conducting the N-terminal sequence analyses and processing the samples for MALDI analysis.

REFERENCES

1. Forst, S., Dowds, B., Boemare, N., and Stackebrandt, E. (1997) *Annu. Rev. Microbiol.* **51,** 47–72
2. Forst, S., and Nealson, K. (1996) *Microbiol. Rev.* **60,** 21–43
3. Tailliez, P., Pagès, S., Ginibre, N., and Boemare, N. (2006) *Int. J. Syst. Evol. Microbiol.* **56,** 2805–2818
4. Waterfield, N. R., Wren, B. W., and Ffrench-Constant, R. H. (2004) *Nat. Rev. Microbiol.* **2,** 833–841
5. Liu, D., Burton, S., Glancy, T., Li, Z. S., Hampton, R., Meade, T., and Merlo, D. J. (2003) *Nat. Biotechnol.* **21,** 1222–1228
6. Bowen, D., Rocheleau, T. A., Blackburn, M., Andreev, O., Golubeva, E., Bhartia, R., and Ffrench-Constant, R. H. (1998) *Science* **280,** 2129–2132
7. ffrench-Constant, R. H., and Bowen, D. J. (2000) *Cell. Mol. Life Sci.* **57,** 828–833
8. Sergeant, M., Jarrett, P., Ousley, M., and Morgan, J. A. (2003) *Appl. Environ. Microbiol.* **69,** 3344–3349
9. Waterfield, N. R., Bowen, D. J., Fetherston, J. D., Perry, R. D., and ffrench-Constant, R. H. (2001) *Trends Microbiol.* **9,** 185–191
10. Ffrench-Constant, R., and Waterfield, N. (2006) *Adv. Appl. Microbiol.* **58,** 169–183
11. ffrench-Constant, R. H., Dowling, A., and Waterfield, N. R. (2007) *Toxicon* **49,** 436–451
12. Heermann, R., and Fuchs, T. M. (2008) *BMC Genomics* **9,** 40
13. Hares, M. C., Hinchliffe, S. J., Strong, P. C., Eleftherianos, I., Dowling, A. J., ffrench-Constant, R. H., and Waterfield, N. (2008) *Microbiology* **154,** 3503–3517
14. Dodd, S. J., Hurst, M. R., Glare, T. R., O'Callaghan, M., and Ronson, C. W. (2006) *Appl. Environ. Microbiol.* **72,** 6584–6592
15. Hurst, M. R., Glare, T. R., Jackson, T. A., and Ronson, C. W. (2000) *J. Bacteriol.* **182,** 5127–5138
16. Guo, L., Fatig, R. O., 3rd, Orr, G. L., Schafer, B. W., Strickland, J. A., Sukhapinda, K., Woodsworth, A. T., and Petell, J. K. (1999) *J. Biol. Chem.* **274,** 9836–9842
17. Lang, A. E., Schmidt, G., Schlosser, A., Hey, T. D., Larrinua, I. M., Sheets,

J. J., Mannherz, H. G., and Aktories, K. (2010) *Science* **327,** 1139–1142
18. Lang, A. E., Schmidt, G., Sheets, J. J., and Aktories, K. (2011) *Naunyn Schmiedebergs Arch. Pharmacol.* **383,** 227–235
19. Laemmli, U. K. (1970) *Nature* **227,** 680–685
20. Wolfersberger, M. G. (1993) *Arch. Insect Biochem. Physiol.* **24,** 139–147
21. Benz, R., Janko, K., Boos, W., and Läuger, P. (1978) *Biochim. Biophys. Acta* **511,** 305–319
22. Lang, A. E., Neumeyer, T., Sun, J., Collier, R. J., Benz, R., and Aktories, K. (2008) *Biochemistry* **47,** 8406–8413
23. Lee, S. C., Stoilova-McPhie, S., Baxter, L., Fülöp, V., Henderson, J., Rodger, A., Roper, D. I., Scott, D. J., Smith, C. J., and Morgan, J. A. (2007) *J. Mol. Biol.* **366,** 1558–1568